THE JOURNAL OF PHYSICAL CHEMISTRY B

Article

pubs.acs.org/JPCB

High Viscosity of Imidazolium Ionic Liquids with the Hydrogen Sulfate Anion: A Raman Spectroscopy Study

Mauro C. C. Ribeiro*

Laboratório de Espectroscopia Molecular, Instituto de Química, Universidade de São Paulo CP 26077, CEP 05513-970, São Paulo, SP, Brazil

ABSTRACT: Ionic liquids based on 1-alkyl-3-methylimidazolium cations and the hydrogen sulfate (or bisulfate) anion, HSO_4^-, are much more viscous than ionic liquids with alkyl sulfates, RSO_4^-. The structural origin of the high viscosity of HSO_4^- ionic liquids is unraveled from detailed comparison of the anion Raman bands in 1-ethyl-3-methylimidazolium hydrogen sulfate and 1-butyl-3-methylimidazolium hydrogen sulfate with available data for simple HSO_4^- salts in crystalline phase, molten phase, and aqueous solution. Two Raman bands at 1046 and 1010 cm^{-1} have been assigned as symmetric stretching modes ν_s(S═O) of HSO_4^-, the latter being characteristic of chains of hydrogen-bonded anions. The intensity of this component increases in the supercooled liquid phase. For comparison purposes, Raman spectra of 1-ethyl-3-methylimidazolium ethyl sulfate and 1-butyl-3-methylimidazolium methyl sulfate have been also obtained. There is no indication of difference in the strength of hydrogen bond interactions of imidazolium cations with HSO_4^- or RSO_4^- anions. Raman spectra at high pressures, up to 2.6 GPa, are also discussed. Raman spectroscopy provides evidence that hydrogen-bonded anions resulting in anion−anion interaction is the reason for the high viscosity of imidazolium ionic liquids with HSO_4^-. If the ionic liquid is exposed to moisture, these structures are disrupted upon absorption of water from the atmosphere.

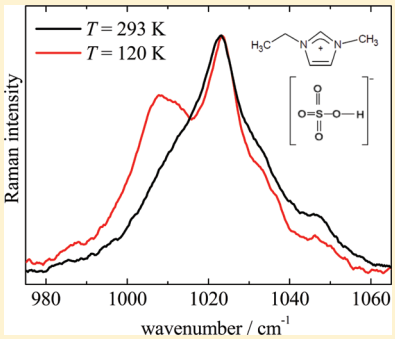

I. INTRODUCTION

Room temperature molten salts, simply called ionic liquids, have been synthesized with many combinations of cations and anions aiming a rational tuning of physicochemical properties, for instance, high conductivity and low viscosity for development of new electrolytes,[1,2] or to improve solvent ability for development of new solvents and extraction media.[3,4] The molecular structures of cation and anion can be systematically modified so that beyond the dominant charge−charge interaction like any simple molten salt, other intermolecular forces such as van der Waals interaction, dipole−dipole, and hydrogen bonding might be decisive to the properties of a given ionic liquid.[5,6] A well-known example of relationship between molecular structure and macroscopic properties is the dependence of transport coefficients of ionic liquids based on 1-alkyl-3-methylimidazolium cations as the length of the alkyl chain increases while keeping the same anion.[7] Viscosity increases and conductivity decreases as the alkyl chain gets longer because van der Waals interactions increase.

Analogous effect has been recently discussed for ionic liquids with a common cation, namely, 1-ethyl-3-methylimidazolium, and alkyl sulfates, RSO_4^-, with increasing length of the anion carbon chain.[8] Interestingly, the ionic liquid with hydrogen sulfate, HSO_4^-, is 1 order of magnitude more viscous than ethyl sulfate, and 2 times more viscous than the octyl sulfate counterparts.[8] Even 1-butyl-3-methylimidazolium methyl sulfate is 10 times less viscous[9] than 1-ethyl-3-methylimidazolium hydrogen sulfate at room temperature. The high viscosity of the HSO_4^- ionic liquid was interpreted as the result of strong cation−anion interaction due to absence of any alkyl chain in the anion.[8] However, analogous systems that have been subject to X-ray structure determination, namely, 1-butyl-2,3-dimethylimidazolium hydrogen sulfate[10] and 1,3-dimethylimidazolium methyl sulfate,[11] exhibit shorter anion−cation distances for the alkyl sulfate derivative, rather than the HSO_4^--based ionic liquid. Although structure determination has been not reported for the ionic liquids considered here, these findings suggest that stronger anion−cation interactions might not be the true reason for the high viscosity of ionic liquids containing the HSO_4^- anion.

The aim of this work is to use Raman spectroscopy to unravel the nature of intermolecular interactions responsible for the high viscosity of imidazolium ionic liquids with HSO_4^-. The schematic structures of the ionic liquids investigated in this work, with their respective notations, are shown in Figure 1: $[C_2C_1Im][HSO_4]$, $[C_4C_1Im][HSO_4]$, $[C_2C_1Im][C_2SO_4]$, and $[C_4C_1Im][C_1SO_4]$. Vibrational spectroscopy has provided important insights on the equilibrium structure, molecular conformations, hydrogen bonding, and ionic pairing in ionic liquids.[12−16] Infrared spectroscopy suggested enhancement of hydrogen bond interactions for $[C_1C_1Im][C_1SO_4]$ under high pressure.[17] There are not as many Raman spectroscopy studies of HSO_4^- ionic liquids as for other common ionic liquids, but in a recent publication concerning $[C_6C_1Im][HSO_4]$, Raman bands assigned to sulfuric acid were observed.[18] The presence of H_2SO_4 was tentatively associated with proton transfer to the

Received: March 2, 2012
Revised: April 26, 2012
Published: May 31, 2012

dx.doi.org/10.1021/jp302091d | J. Phys. Chem. B 2012, 116, 7281−7290

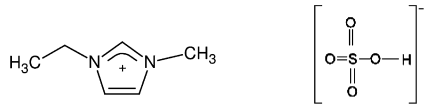

1-ethyl-3-methylimidazolium hydrogen sulphate, $[C_2C_1Im][HSO_4]$

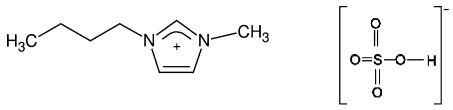

1-butyl-3-methylimidazolium hydrogen sulphate, $[C_4C_1Im][HSO_4]$

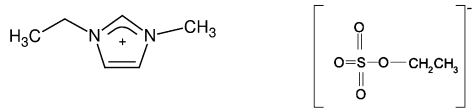

1-ethyl-3-methylimidazolium ethylsulphate, $[C_2C_1Im][C_2SO_4]$

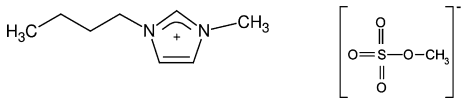

1-butyl-3-methylimidazolium methylsulphate, $[C_4C_1Im][C_1SO_4]$

Figure 1. Ionic structures and notation of the systems investigated in this work.

HSO_4^- anion, even though the origin of this proton transfer was not clear.[18] In this work, however, no H_2SO_4 bands were observed in the Raman spectra of $[C_2C_1Im][HSO_4]$ and $[C_4C_1Im][HSO_4]$ as previously found in $[C_6C_1Im][HSO_4]$.[18]

The HSO_4^- anion is a simple species for which many Raman spectroscopy investigations of salts with ammonium or alkali metal cations are available for aqueous solution,[19−24] crystal,[25−28] and (high temperature) molten salt.[29,30] The most important Raman bands for this work correspond to ν_s(S═O) and ν(S−OH) modes, since the vibrational frequencies depend on temperature and local environment around the HSO_4^- anion. Raman spectroscopy has been used to study solid−solid phase transitions of HSO_4^- salts because of their interesting superprotonic phases, in which reorientational disorder at high temperatures allows for fast proton transfer between anions in the solid phase.[26−28] Structure determination of simple HSO_4^- salts indicated infinite chains of hydrogen-bonded anions, $(HSO_4^-)_n$, in the low-temperature crystal, which are disrupted into dimers $(HSO_4^-)_2$ as temperature increases.[31−35] More recently, X-ray diffraction measurements showed the occurrence of $(HSO_4^-)_2$ dimers in $[C_1C_1Im][HSO_4]$ single crystal.[11] The high viscosity of (high temperature) molten phases of simple HSO_4^- salts has been already interpreted six decades ago by these structures of hydrogen-bonded anions remaining in the liquid just above the melting temperature.[36] Raman spectra obtained in this work for ionic liquids in the range of the ν_s(S═O) mode exhibit the component assigned to chains of HSO_4^- ions. A characteristic feature of ionic liquids that is also interesting for this work is that many of them are easily supercooled upon reduction of temperature below T_m, with typical glass transition at $T_g \sim 200$ K.[37−40] Therefore, it is possible to investigate the Raman signature of these structures in the amorphous phase at very low temperature. Furthermore, by changing temperature and pressure, one is able to discriminate between thermal and density effects on vibrational frequency, relative intensity, and bandwidth.

II. EXPERIMENTAL SECTION

The ionic liquids $[C_2C_1Im][HSO_4]$ and $[C_4C_1Im][HSO_4]$ were purchased from Iolitec, $[C_2C_1Im][C_2SO_4]$ from Solvent Innovations, and $[C_4C_1Im][C_1SO_4]$ from Sigma-Aldrich. The ionic liquids were dried under high vacuum (below 10^{-5} mbar) for several days before measurements. Raman spectra as a function of temperature were recorded with a Jobin-Yvon T64000 triple monochromator spectrometer equipped with CCD. The spectra were excited with the 647.1 nm line of a Coherent Innova 90 Kr^+ laser, and the spectral resolution was 2.0 cm^{-1}. Raman spectra as a function of temperature were obtained in the usual 90° scattering geometry, and temperature control was achieved with the Optistat DN cryostat of Oxford Instruments. Raman spectra as a function of pressure at room temperature were obtained with a Renishaw inVia, fitted with a CCD camera, and coupled to a Leica microscope. The 632.8 nm line from a He−Ne laser was focused onto the sample by a 20× Leica objective. High-pressure measurements were performed with a diamond anvil cell from EasyLab Technologies Ltd., model Diacell Bragg-XVue, having a diamond culet size of 500 μm. The Boehler microDriller (EasyLab) was used to drill a 250 μm hole in a stainless steel gasket (10 mm diameter, 250 μm thick) preindented to ∼150 μm. The ionic liquid sample is also the compressing medium with no need of adding another liquid. Pressure calibration was done by the usual method of measuring the shift of the fluorescence line of a ruby sphere added to the sample chamber.

III. RESULTS AND DISCUSSION

A. Overview of the Raman Spectra. Raman spectra of $[C_2C_1Im][HSO_4]$ and $[C_4C_1Im][HSO_4]$ at room temperature and pressure are shown in Figure 2. In molten $KHSO_4$, Raman spectroscopy showed that bands characteristic of $S_2O_7^{2-}$ appear as temperature increases due to the reaction $2HSO_4^- \rightarrow S_2O_7^{2-} + H_2O$.[29,30] This reaction starts at relatively high temperature (above 573 K), so that the presence of $S_2O_7^{2-}$ is not an issue here since we will work with ionic liquids at temperatures not

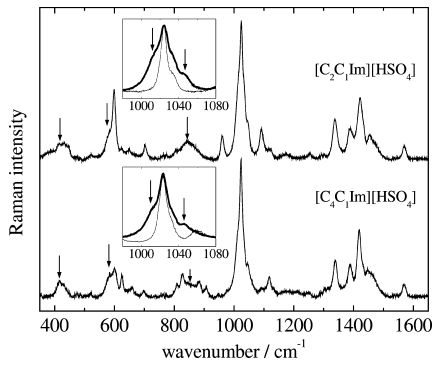

Figure 2. Raman spectra of $[C_2C_1Im][HSO_4]$ (top) and $[C_4C_1Im]$-$[HSO_4]$ (bottom) at room temperature and pressure. Insets compare the 980−1080 cm^{-1} range of the Raman spectra of $[C_2C_1Im][HSO_4]$ and $[C_2C_1Im]Cl$ (bold and thin lines in top inset, respectively), and $[C_4C_1Im][HSO_4]$ and $[C_4C_1Im]Br$ (bold and thin lines in bottom inset, respectively). Arrows indicate Raman bands of the HSO_4^- anion listed in Table 1.

dx.doi.org/10.1021/jp302091d | J. Phys. Chem. B 2012, 116, 7281−7290

higher than 400 K. In a previous study concerning $[C_6C_1Im][HSO_4]$,[18] Raman bands assigned to H_2SO_4 have been observed. In this work, however, we have not found H_2SO_4 bands in the Raman spectra of $[C_2C_1Im][HSO_4]$ and $[C_4C_1Im][HSO_4]$. In ref 18, there was not a definitive conclusion whether the H_2SO_4 was simply residual from the $[C_6C_1Im][HSO_4]$ synthesis or there was proton transfer from a neighboring species (imidazolium cation, anion, or water) to HSO_4^-. Raman spectroscopy investigation of concentrated sulfuric acid[24] assigned the symmetric and asymmetric stretching modes of H_2SO_4 at ν_s(S−OH) = 905 cm^{-1}, ν_{as}(S−OH) = 970 cm^{-1}, ν_s(S═O) = 1165 cm^{-1}, and ν_{as}(S═O) = 1350 cm^{-1}. The absence of these bands in the Raman spectra obtained in this work for ionic liquids analogous to $[C_6C_1Im][HSO_4]$ suggests that most probably there was residual of sulfuric acid in the sample used in ref 18.

The most intense band in Raman spectra of imidazolium ionic liquids with relatively simple polyatomic anions, e.g., BF_4^-, PF_6^-, NO_3^-, usually corresponds to the totally symmetric normal mode of the anion, but this is not the case for $[C_2C_1Im][HSO_4]$ and $[C_4C_1Im][HSO_4]$. Despite overlaps between anion and cation bands, the HSO_4^- bands can be identified by comparing Raman spectra of ionic liquids with the same cation and other anions, in particular, halide anions. Table 1 gives vibrational frequencies assigned to HSO_4^- normal modes in the ionic liquids investigated in this work. There are no differences of HSO_4^- vibrational frequencies between $[C_2C_1Im][HSO_4]$ and $[C_4C_1Im][HSO_4]$. The long list of vibrational frequencies of $[C_2C_1Im]^+$ and $[C_4C_1Im]^+$ is not given in Table 1 because vibrational spectra and quantum chemistry calculations of imidazolium cations with many different anions have been extensively discussed in several works.[12−16]

Table 1. Comparison of Raman Shifts (cm^{-1}) of HSO_4^- Normal Modes Obtained in This Work for the Ionic Liquids $[C_2C_1Im][HSO_4]$ and $[C_4C_1Im][HSO_4]$ at Room Pressure and Temperature, and Literature Data for Simple HSO_4^- Salts in Different States

ionic liq (this work)	molten $KHSO_4$ 480 < T < 723 K[a]	NH_4HSO_4 aq soln[b]	$CsHSO_4$ cryst, 423 K[c]	assignment (C_{3v} sym)
416	417	422	423	$\delta_{as}(SO_3)$, E
581	585	586	589	$\delta_s(SO_3)$, A_1
845	844−823	898	838	ν(S−OH), A_1
1010			995	ν_s(S═O),[d] A_1
1046	1046	1052	1036	ν_s(S═O), A_1
	1205		1214	ν_{as}(S═O), E

[a]Reference 30. [b]0.876 *m*, room temperature, ref 22. [c]Reference 28. [d]Hydrogen-bonded anions in $(HSO_4^-)_n$ chains.

Raman spectra of molten $KHSO_4$ reported in refs 29 and 30 (see Table 1) were interpreted on the basis of a C_s symmetry for HSO_4^-. Broad and weak bands around 1360−1390 cm^{-1} observed in ref 29 were not observed in ref 30. Bands above 3000 cm^{-1} were not assigned to HSO_4^-; instead, these O−H stretching modes were assigned to H_2O resulting from decomposition of the anion.[30] Raman bands of S−O−H bending modes are also weak and most probably are responsible for broad features within the 1100−1300 cm^{-1} range.[30] The insets in Figure 2 compare Raman spectra within the 980−1080 cm^{-1} range of $[C_2C_1Im][HSO_4]$ and $[C_2C_1Im]$Cl (top inset), and $[C_4C_1Im][HSO_4]$ and $[C_4C_1Im]$Br (bottom inset). The HSO_4^- bands overlap with modes of the imidazolium ring at 1022 cm^{-1} with a shoulder at 1033 cm^{-1} that are also observed in $[C_2C_1Im]$Cl and $[C_4C_1Im]$Br.[16] The additional bands observed in this range of the Raman spectra of $[C_2C_1Im][HSO_4]$ and $[C_4C_1Im][HSO_4]$ are indicated in Figure 2 by arrows at 1010 and 1046 cm^{-1}.

The Raman band observed at 1010 cm^{-1} in the ionic liquids corresponds to the lower frequency component of the ν_s(S═O) mode of HSO_4^- previously seen in crystalline phases of simple HSO_4^- salts (see Table 1), and assigned to hydrogen-bonded anions in structures like chains, $(HSO_4^-)_n$.[25−28] Raman spectroscopy provides signatures of HSO_4^- in different environments: in solid $KHSO_4$ at room temperature, the totally symmetric stretching mode ν_s(S═O) exhibits two components at 1001 and 1026 cm^{-1} that are assigned to anions in structures of chains and dimers, respectively.[25] In solid $CsHSO_4$, the ν_s(S═O) mode is observed at 999 cm^{-1} at room temperature due to $(HSO_4^-)_n$ chains, shifting to 1024 cm^{-1} at 340 K due to formation of $(HSO_4^-)_2$ dimers, and 1036 cm^{-1} at 417 K in the superprotonic phase in which reorientational disorder results in broad bands.[26,28] This sequence of weakening of hydrogen bonds in $CsHSO_4$ as temperature increases can be also followed by the ν(S−OH) mode: 863 cm^{-1} (300 K < T < 340 K), 852 cm^{-1} (350 K < T < 417 K), and 838 cm^{-1} (417 K < T < T_m = 484 K).[26,28] There are two hydrogen bonds in a $(HSO_4^-)_2$ dimer, in which each anion of the pair is accepting and donating a hydrogen bond to the other anion. In the infinite $(HSO_4^-)_n$ chain, a given anion donates and accepts hydrogen bonds to two different neighboring anions. The difference of vibrational frequencies between chains and dimers of HSO_4^- comes from the different strengths of hydrogen bonds, as indicated by the O···O distance between two hydrogen-bonded anions in chains and dimers, respectively, 2.573 and 2.619 Å (see sketches of chain and dimer structures in ref 25).

The spectral signature of structures like $(HSO_4^-)_n$ has been discussed in crystalline phases of HSO_4^- salts,[25−28] but not in molten $KHSO_4$.[29,30] Finding the spectral feature related to relatively long structures of hydrogen-bonded anions in HSO_4^- ionic liquids is reasonable because the temperature of the ionic liquid is 200 K lower than that of molten $KHSO_4$. On the other hand, the 1046 cm^{-1} band in the ionic liquids (see insets of Figure 2) is the component analogous to that observed in molten $KHSO_4$ corresponding to the ν_s(S═O) mode of HSO_4^- interacting with neighboring cations and anions, eventually forming $(HSO_4^-)_2$ dimers.[25−30]

Table 1 allows for interesting comparisons of the vibrational frequencies of ν(S−OH) and ν_s(S═O) modes in different environments that give preliminary insights on ionic interactions in ionic liquids. In aqueous solution, relative intensities of characteristics Raman bands have been used to address the temperature dependence of the equilibrium $HSO_4^- + H_2O \rightarrow SO_4^{2-} + H_3O^+$,[19−22] and the first dissociation step $H_2SO_4 + H_2O \rightarrow HSO_4^- + H_3O^+$ in concentrated sulfuric acid.[23,24] In solution, Raman spectra have been interpreted on the basis of a C_{3v} symmetry for the HSO_4^- species, O*−SO_3, i.e., the OH considered as united group.[20−24] The same vibrational frequencies of HSO_4^- have been obtained for salts with different cations,[19] but ν(S−OH) and ν_s(S═O) depend on concentration.[19−24] For instance, in a 15.53 *m* aqueous solution of NH_4HSO_4 at 295 K, ν(S−OH) and ν_s(S═O) are observed at 888 and 1046 cm^{-1}, respectively.[22] There is a

dx.doi.org/10.1021/jp302091d | J. Phys. Chem. B 2012, 116, 7281−7290

remarkable temperature dependence of ν(S−OH) in solution: it decreases from ∼900 cm^{-1} at 273 K to ∼845 cm^{-1} at 550 K.[21,22,24] In molten $KHSO_4$, ν(S−OH) is also inversely dependent on temperature: the Raman shift increases from 823 to 844 cm^{-1} as temperature decreases from 723 to 480 K.[30] All of these findings in crystals, melts, and aqueous solutions of simple HSO_4^- salts mean that S−OH bond strengths and S═O bonds weaken upon formation of hydrogen bond, which is expected to be stronger between HSO_4^- and charged species (e.g., cations, H_3O^+ or a neighboring HSO_4^- anion) than HSO_4^- and neutral species (e.g., H_2O or H_2SO_4).

Wavenumbers for the ν(S−OH) and ν_s(S═O) modes in ionic liquids, respectively, 845 and 1046 cm^{-1}, are different from the HSO_4^- vibrational frequencies in aqueous solution at room temperature. The HSO_4^- vibrational frequencies in ionic liquids correspond to values observed in molten $KHSO_4$ (see Table 1). The ν(S−OH) in ionic liquids at room temperature compares with molten $KHSO_4$ just above the melting temperature, in spite of a temperature difference of ca. 200 K between these data. The finding of essentially the same HSO_4^- vibrational frequencies in ionic liquids and molten $KHSO_4$ is remarkable in light of the complex molecular structure of imidazolium cations. This strongly suggests that HSO_4^- vibrational frequencies observed in both the high-temperature and the room-temperature molten salts depend more on anion−anion interaction than any specific HSO_4^-−imidazolium interaction, such as anion−cation hydrogen bond.

Figure 3 shows the 930−1170 cm^{-1} frequency range of Raman spectra of the alkyl sulfates ionic liquids $[C_2C_1Im]$-$[C_2SO_4]$ and $[C_4C_1Im][C_1SO_4]$. The Raman spectrum of $[C_2C_1Im][C_2SO_4]$ obtained in this work agrees with previous results for this ionic liquid.[41,42] In alkyl sulfate ionic liquids, the ν_s(S═O) mode gives an intense and sharp band at 1060 cm^{-1}. The ν_s(S═O) mode at 1010 cm^{-1} is also observed as a shoulder in the Raman spectrum of the ionic liquid containing the methyl sulfate anion, but not in the ethyl sulfate derivative (see Figure 3). Thus, anion−anion interaction also occurs between $CH_3SO_4^-$ anions, but not between anions with longer carbon chains such as $CH_3CH_2SO_4^-$.

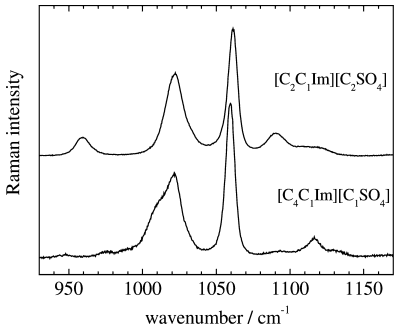

Figure 3. Raman spectra of $[C_2C_1Im][C_2SO_4]$ (top) and $[C_4C_1Im]$-$[C_1SO_4]$ (bottom) at room temperature and pressure.

Despite the simple molecular structure of the HSO_4^- anion, it should be noticed there are some features far from trivial in Raman spectra of HSO_4^- salts. In aqueous solution of simple HSO_4^- salts, the ν_s(S═O) mode at ∼1050 cm^{-1} exhibits a low-frequency asymmetry at ∼1035 cm^{-1}, for which different interpretations have been proposed, such as distinct coordination structures of water molecules around the HSO_4^-,[20] nonequivalence of the S═O bonds,[21] or hydrogen bond between anions.[22] The occurrence of relatively well-defined structures like $(HSO_4^-)_2$ dimers is also suggested from the finding of the noncoincidence effect; i.e., the frequencies of the peak of the ν_s(S═O) band in polarized and depolarized Raman spectra do not coincide. In a 15.530 *m* solution of NH_4HSO_4 at room temperature, the peaks of polarized and depolarized spectra are observed at 1046 and 1053 cm^{-1}, respectively, and the noncoincidence effect disappears in diluted solution.[22] The noncoincidence effect has a long history in Raman spectroscopy of liquids,[43−46] being usually observed for a normal mode with large transition dipole, i.e., a normal mode giving an intense band in the infrared spectrum. The origin of the noncoincidence effect is interaction between oscillators in an orientationally ordered structure of two neighboring molecules. In other words, the noncoincidence effect in Raman spectroscopy is a signature of short-ranged structures in liquid phase.[43−46]

The study of temperature and pressure effects will reinforce the preliminary conclusions drawn from Raman spectra of HSO_4^- ionic liquids at room condition. However, before further analysis of the HSO_4^- bands, the next section addresses the high frequency range related to C−H stretching modes. Although the assignment of normal modes in this range is not straightforward, the high-frequency range of Raman spectra of ionic liquids has been used to unravel the strength of hydrogen bonds between imidazolium cations and different anions.[12,14−17] Thus, it is worth investigating whether the origin of the high viscosity of HSO_4^- ionic liquids is due to the distinct strength of interaction between the cation and HSO_4^- or RSO_4^- anions.

B. Frequency Range of the C−H Stretching Modes. Figure 4 shows the high-frequency range of Raman spectra of $[C_2C_1Im][HSO_4]$, $[C_2C_1Im][C_2SO_4]$, $[C_4C_1Im][HSO_4]$, and $[C_4C_1Im][C_1SO_4]$ at room temperature and pressure. Raman spectra in this frequency range are essentially the same for these ionic liquids, with only slight differences in the group of bands within the 2850−3000 cm^{-1} range related to C−H stretching modes of the alkyl chains. Bands above 3000 cm^{-1}, assigned to C−H stretching modes of the imidazolium ring, have been used as probes of the strength of hydrogen bonds, shifting to lower wavenumbers as more basic is the anion.[12,14−16] It is clear from Figure 4 that the two bands related to C−H stretching modes of the imidazolium ring have the same Raman shifts in these ionic liquids, 3109 and 3165 cm^{-1}. For comparison purposes, these bands are observed at 3070 and 3150 cm^{-1} in the ionic liquid $[C_4C_1Im]Br$ at T = 360 K.[16] In this doublet of bands, the

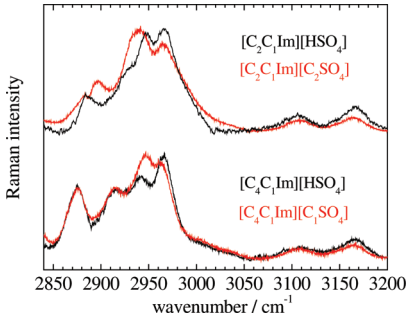

Figure 4. Raman spectra in the range of the C−H stretching modes of $[C_2C_1Im][HSO_4]$ and $[C_2C_1Im][C_2SO_4]$ (black and red lines at top), and $[C_4C_1Im][HSO_4]$ and $[C_4C_1Im][C_1SO_4]$ (black and red lines at bottom), at room temperature and pressure.

dx.doi.org/10.1021/jp302091d | J. Phys. Chem. B 2012, 116, 7281−7290

lower frequency component is usually assigned to C−H stretching of the carbon atom between the nitrogen atoms of the imidazolium ring, i.e., the carbon atom $C_{(2)}$. The higher frequency component is thus assigned to C−H stretching modes of the atoms $C_{(4)}$ and $C_{(5)}$ of the ring. The finding of $C_{(2)}$−H frequency lower than $C_{(4,5)}$−H frequency is considered a signature of the more acidic character of the hydrogen atom bonded to the $C_{(2)}$ atom, allowing for hydrogen bond $C_{(2)}$—H···X^- stronger than $C_{(4,5)}$—H···X^-. The same vibrational frequencies of this doublet of bands, 3109 and 3165 cm^{-1}, in ionic liquids with either HSO_4^- or RSO_4^-, strongly suggest there is no difference in the strength of hydrogen bonds between imidazolium cations and each of these anions.

In a previous infrared spectroscopy investigation of $[C_1C_1Im][C_1SO_4]$ under high pressure, it has been found that vibrational frequencies of C−H stretching modes decrease for pressures up to 1.0 GPa, and then increase for higher pressures.[17] The initial drop of vibrational frequencies with increasing pressure for some C−H bands was interpreted as stabilization of anion−cation hydrogen bonds.[17] Figure 5 shows

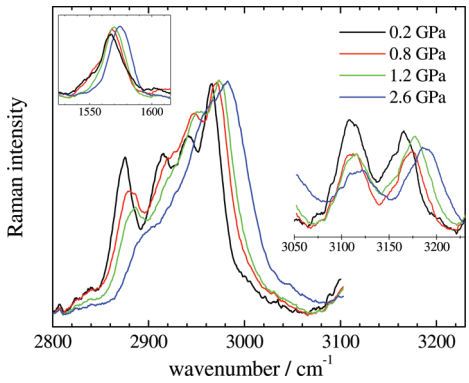

Figure 5. Pressure dependence of Raman spectra in the range of the C−H stretching modes of $[C_4C_1Im][HSO_4]$ at room temperature. The spectra within 3050−3230 cm^{-1} range are shown in an enlarged scale. The upper inset shows the pressure dependence of ∼1570 cm^{-1} band of a ring mode.

Raman spectra as a function of pressure in the range of C−H stretching modes of $[C_4C_1Im][HSO_4]$ at room temperature. Corresponding data for the others ionic liquids investigated in this work are not shown since similar pressure effect has been found as illustrated for $[C_4C_1Im][HSO_4]$. Pressure effect on peak positions is clear in Figure 5, in contrast to essentially the same band profile in this frequency range when cooling the system to the supercooled liquid phase (data not shown). Figure 6 shows that a good fit to the whole 2800−3200 cm^{-1} spectral range is achieved with six Lorentzian bands. The same number of components also gives a good fit to the high-pressure spectrum, in which each component becomes broader and overlaps in an overall less structured band profile.

Contrary to ref 17, we found that peak positions of all of the components in the range of C−H stretching modes increase with pressure for the ionic liquids investigated in this work. It is worth noting the significant changes on band profiles of the infrared spectra of $[C_1C_1Im][C_1SO_4]$ shown in Figure 1 of ref 17, including splitting of bands at high pressures, but unfortunately best fits to experimental data have not been shown in ref 17. In this work, we observed just the expected blue shift of the vibrational frequency as the oscillator probes the short-range repulsive part of the intermolecular potential

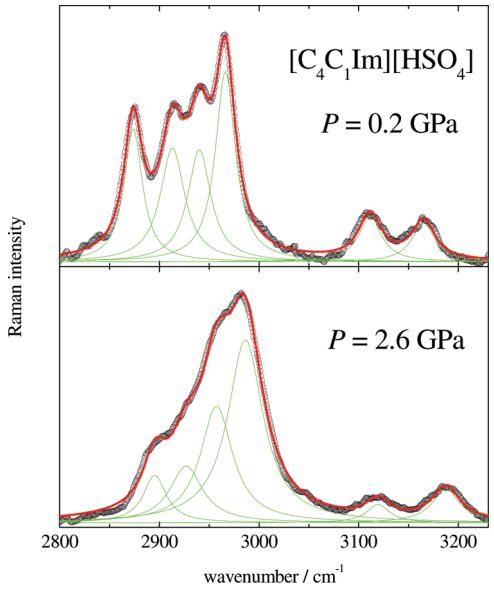

Figure 6. Raman spectra at 0.2 GPa (top) and 2.6 GPa (bottom) at room temperature in the range of the C−H stretching modes of $[C_4C_1Im][HSO_4]$ (black dots). The red lines on the experimental data are best fits with the Lorentzian functions shown as green lines. The parameters (center/width) in cm^{-1} for each Lorentzian component are (2873/22), (2913/30), (2940/28), (2966/24), (3111/27), and (3165/28) in the top panel; (2895/28), (2926/40), (2957/39), (2986/43), (3120/28), and (3187/33) in the bottom panel.

with increasing density. Therefore, we found no indication of stabilization of C—H···O hydrogen bonds under high pressure as claimed in ref 17.

The frequency range above 3050 cm^{-1} is shown in Figure 5 in an enlarged scale for helping visualization of the pressure effect on the doublet of bands for which an alternative interpretation has been proposed.[14,16] Rather than assigning one band to $C_{(2)}$−H and the other one to $C_{(4,5)}$−H stretching, it was proposed that this doublet of bands comes from Fermi resonance between fundamental C−H stretching modes and the first overtone of ring modes at 1500−1600 cm^{-1}. The Raman band at ∼1570 cm^{-1} shown in the inset of Figure 5 corresponds to the imidazolium ring mode whose overtone is supposed to be in Fermi resonance with C−H fundamentals. This new interpretation is a strong suggestion because it is a warning on using this range of vibrational spectra to draw conclusions about preferred sites for hydrogen bonding to the imidazolium ring.[14−16] The proposition of Fermi resonance was based on infrared and Raman spectroscopy studies of ionic liquids with different anions and 1-alkyl-3-methylimidazolium cations in which selective isotopic substitutions of the hydrogen atoms have been done. It should be noted that application of pressure is another procedure to show whether Fermi resonance is a reasonable assignment, since frequency shift with increasing pressure might be of different magnitude for each of the two states supposed to be in Fermi resonance.[47−50] In a favorable case, one could eventually discriminate between different assignments by recording Raman spectra as a function of pressure.

Although a full investigation about the controversy on the assignment of the high-frequency range of vibrational spectra of imidazolium ionic liquids is beyond the scope of this work, we found on the basis of high-pressure data that a simple model of two modes in Fermi resonance is a valid interpretation for the

dx.doi.org/10.1021/jp302091d | J. Phys. Chem. B 2012, 116, 7281−7290

ionic liquids considered here. Figure 7 shows frequency shifts as a function of pressure for $[C_4C_1Im][HSO_4]$ in relation to the

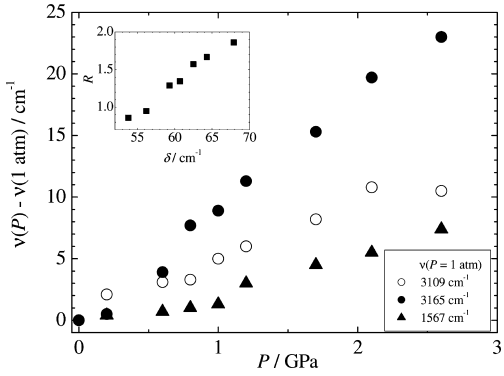

Figure 7. Frequency shift of Raman bands of $[C_4C_1Im][HSO_4]$ relative to values at room pressure: 1567 cm^{-1} (black triangles), 3109 cm^{-1} (white circles), and 3165 cm^{-1} (black circles). The inset shows the intensity ratio, $R = I_+/I_-$, as a function of the frequency separation, $\delta = \nu_+ - \nu_-$, of the C−H stretching modes assumed in Fermi resonance.

room condition value, $\nu(P) - \nu(P{=}1\ atm)$. Pressure effect on the peak position of the fundamental band at 1567 cm^{-1} is also shown in Figure 7. Pressure increases the separation of the doublet, $\delta = \nu_+ - \nu_-$, where ν_+ and ν_- are respectively the higher and the lower frequency component of the doublet, i.e., the Raman bands at 3165 and 3109 cm^{-1} at room pressure. Inset of Figure 7 shows that the ratio of intensities of the two components, $R = I_+/I_-$, increases with δ as pressure increases. The finding that I_- decreases as δ increases is consistent with assigning the lower frequency component of the doublet as the overtone of the imidazolium ring mode at 1567 cm^{-1}. Assuming a simple model of two states in Fermi resonance, the separation of the states unperturbed by Fermi resonance, δ_0, and the coefficient of Fermi resonance coupling, W, can be estimated by $\delta_0 = (\delta^2 - 4W^2)^{1/2}$, where $W = \delta R^{1/2}(1 + R)^{-1}$.[49] The experimental values of δ and R for $[C_4C_1Im][HSO_4]$ shown in the inset of Figure 7 give the unperturbed separation of the two states in the range $2 < \delta_0 < 20$ cm^{-1}, and the coefficient coupling $26 < W < 32$ cm^{-1}, from room pressure up to 2.6 GPa. For comparison purposes, the parameter W is similar to obtained in liquid dichloromethane and about half the value in liquid methanol,[49] but the Fermi resonance interaction in the ionic liquid should be considered strong proper to the small separation δ_0 between the states.

In summary, pressure dependence of the doublet of bands above 3000 cm^{-1} in the Raman spectrum of $[C_4C_1Im][HSO_4]$ is consistent with the proposition of two states mixed by Fermi resonance, although not being a proof of this interpretation. Work is in progress to extend the analysis of Fermi resonance as a function of pressure for other imidazolium ionic liquids aiming to find similar values of the Fermi resonance coupling coefficient that could reinforce such interpretation. Nevertheless, whether Fermi resonance is the correct assignment or not for the bands observed around 3100 cm^{-1} in vibrational spectra of imidazolium ionic liquids, there is an overall agreement that the positions of these bands are good probes of the strength of hydrogen bonds between anions and imidazolium cations.[15] The finding of the same vibrational frequencies for the imidazolium cations in ionic liquids containing either HSO_4^- or alkyl sulfates supports the reasoning that the difference in viscosity between these liquids does not arise from differences in the strength of interactions between the cation and each of these anions. The analysis of the HSO_4^- bands in the next section gives a hint on the nature of the anion−anion interaction, and the resulting microscopic structure that is on the basis of the high viscosity of HSO_4^- ionic liquids.

C. Temperature and Pressure Effects on the Anions Vibrational Modes. Figure 8 shows the frequency range of

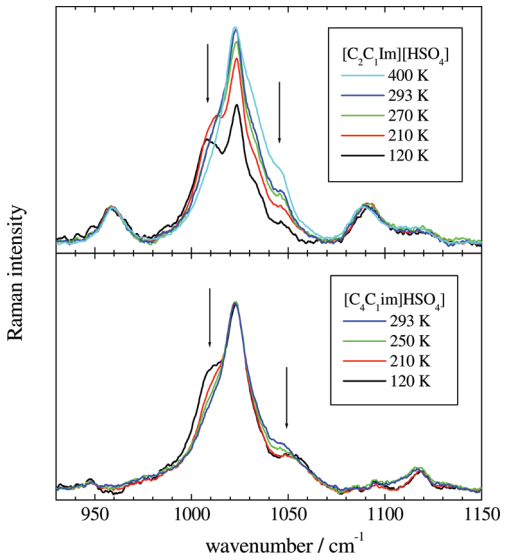

Figure 8. Temperature dependence of Raman spectra in the range of the ν_s(S═O) mode of $[C_2C_1Im][HSO_4]$ (top) and $[C_4C_1Im][HSO_4]$ (bottom) at room pressure. The arrows indicate ν_s(S═O) bands of the hydrogen sulfate anion.

the ν_s(S═O) stretching mode of the Raman spectra of $[C_2C_1Im][HSO_4]$ and $[C_4C_1Im][HSO_4]$ in the normal liquid, supercooled liquid, and glassy phases. Raman spectra of $[C_2C_1Im][HSO_4]$ at different temperatures have been normalized by the intensities of bands at 960, 1090, and 1120 cm^{-1} belonging to the $[C_2C_1Im]^+$ moiety, while Raman spectra of $[C_4C_1Im][HSO_4]$ have been simply normalized by their maxima. The relative intensities of ν_s(S═O) stretching modes at 1010 and 1046 cm^{-1} indicated by arrows in Figure 8 have opposite temperature dependence. This is clearer in Figure 9, which shows two examples of fits to Raman spectra for $[C_2C_1Im][HSO_4]$ at 293 and 120 K. The band observed only as a shoulder at 1010 cm^{-1} at room temperature, which overlaps the imidazolium ring modes at 1022 and 1033 cm^{-1}, shifts to lower wavenumber as temperature decreases, becoming a well-defined band at low temperature. In contrast, the relative intensity of the ν_s(S═O) mode at 1046 cm^{-1} decreases as temperature decreases. The temperature dependence of the band at 1010 cm^{-1} is the expected behavior for the ν_s(S═O) mode of hydrogen-bonded anions in structures like $(HSO_4^-)_n$ chains as observed in crystalline phases of $KHSO_4$ and $CsHSO_4$.[25−28] It is worth noting that the top panel in Figure 8 includes a Raman spectrum of $[C_2C_1Im][HSO_4]$ at 400 K, in which the ν_s(S═O) mode related to $(HSO_4^-)_n$ chains still remains as an asymmetry in the low-frequency side of the main band. The Raman spectra in the bottom panel of Figure 8 give the same physical picture for $[C_4C_1Im][HSO_4]$. It would be interesting for future works to investigate whether longer side chains in 1-alkyl-3-methylimidazolium cations, say

dx.doi.org/10.1021/jp302091d | J. Phys. Chem. B 2012, 116, 7281−7290

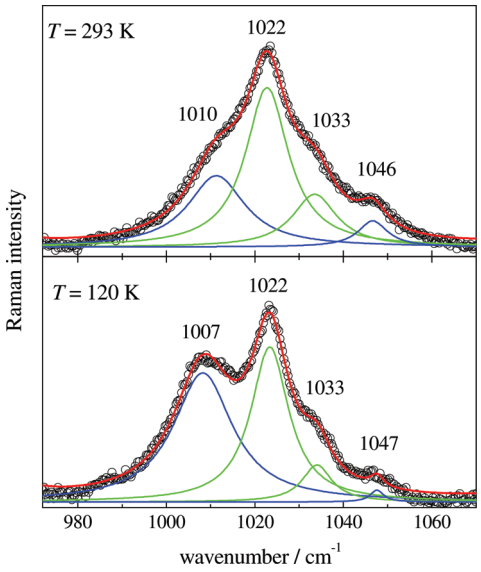

Figure 9. Raman spectra at room temperature (top) and 120 K (bottom) at room pressure in the range of ν_s(S═O) modes of $[C_2C_1Im][HSO_4]$ (black dots). The red lines on the experimental data are best fits with the Lorentzian functions shown as green and blue lines (the components in blue correspond to HSO_4^- normal modes).

$[C_6C_1Im]^+$, $[C_8C_1Im]^+$, etc., have the effect of blocking the formation of $(HSO_4^-)_n$ chains in these ionic liquids.

The contrast between the temperature effect on Raman spectra of $[C_2C_1Im][HSO_4]$ and $[C_2C_1Im][C_2SO_4]$ is clear when one compares the top panels of Figures 8 and 10. The Raman spectrum of $[C_2C_1Im][C_2SO_4]$ in Figure 10 is essentially temperature independent. The band assigned to the ν_s(S═O) mode at 1060 cm^{-1} becomes sharper as the system goes to the supercooled liquid and glassy state, but there is no frequency shift. We found that only the $\delta_s(SO_3)$ bending mode of $[C_2C_1Im][C_2SO_4]$ at 765 cm^{-1} exhibits blue shift at low temperature (compare the black and red lines in the upper inset of Figure 10). However, the temperature dependence of the $\delta_s(SO_3)$ mode of $[C_2SO_4]^-$ is not necessarily a thermal effect; instead, it is due to increasing density as temperature decreases. In fact, a slight increase of pressure at room temperature keeps the whole Raman spectrum of $[C_2C_1Im]$-$[C_2SO_4]$ unchanged except by an upward shift of the $\delta_s(SO_3)$ band (green line in the top inset of Figure 10).

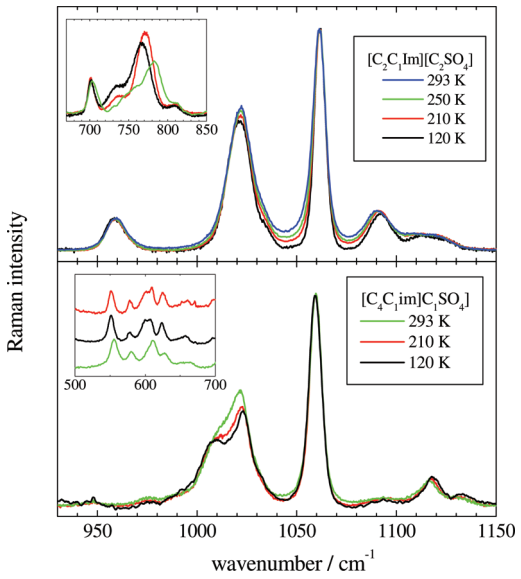

Figure 10. Temperature dependence of Raman spectra in the range of the ν_s(S═O) mode of $[C_2C_1Im][C_2SO_4]$ (top) and $[C_4C_1Im]$-$[C_1SO_4]$ (bottom) at room pressure. The upper inset compares Raman spectra in the range of the bending $\delta(SO_3)$ mode of $[C_2C_1Im][C_2SO_4]$ at room temperature and pressure (black), room pressure and T = 210 K (red), and room temperature and P = 0.2 GPa (green). The lower inset compares Raman spectra in the range of modes related to conformations of the butyl chain of $[C_4C_1Im]$-$[C_1SO_4]$ at room temperature and pressure (black), room pressure and T = 120 K (red), and room temperature and P = 1.8 GPa (green).

Temperature dependence of Raman spectra of $[C_4C_1Im]$-$[C_1SO_4]$ shown in the bottom panel of Figure 10 suggests that anion−anion interaction is taking place between $[C_1SO_4]^-$ anions. The Raman band shape of the ν_s(S═O) mode at 1060 cm^{-1} does not change by cooling $[C_4C_1Im][C_1SO_4]$, but the 1010 cm^{-1} component is a resolved band at low temperature in analogy to Raman spectra of HSO_4^- ionic liquids. Therefore, structures made of hydrogen-bonded $[C_1SO_4]^-$ anions are also formed, most probably involving not too many units as long $(HSO_4^-)_n$ chains, but are not formed between $[C_2SO_4]^-$ because of the longer alkyl chain. For completeness, the bottom inset of Figure 10 shows the 500−800 cm^{-1} range of Raman spectra of $[C_4C_1Im][C_1SO_4]$. Relative intensities of Raman bands in this spectral range have been considered as probes of relative population of *anti−anti* and *gauche−anti* conformers of the butyl chain in $[C_4C_1Im]^+$.[12,51−54] Similar band profiles seen in the bottom inset of Figure 10 suggest there is no significant modification of the population of conformers at different conditions of temperature and pressure for the ionic liquid $[C_4C_1Im]$-$[C_1SO_4]$.

In crystalline phases of $CsHSO_4$, it has been shown that absorption of water or mechanical treatment destroys the long chains of hydrogen-bonded anions into shorter chains or $(HSO_4^-)_2$ dimers.[27] This result suggested an additional check on the validity of corresponding assignment of ν_s(S═O) modes at 1010 and 1046 cm^{-1} in HSO_4^- ionic liquids. A sample of $[C_2C_1Im][HSO_4]$ was left in an opened glass tube (3 mm diameter, 40 mm length) exposed to the moisture, so that the ionic liquid could absorb water from atmosphere. After a few days, Raman spectra were obtained by focusing the laser beam close to the surface of the liquid or at the bottom of the liquid. Figure 11 shows the frequency range including the ν(S−OH) and ν_s(S═O) modes for these two spectra normalized by intensities of $[C_2C_1Im]^+$ modes at 960, 1090, and 1120 cm^{-1}. It is clear from Figure 11 the remarkable change of band shape in the 1000−1060 cm^{-1} range. It is worth stressing that both the spectra in Figure 11 correspond to the same sample of $[C_2C_1Im][HSO_4]$; the difference is only the position of the laser beam in different parts of the liquid. In the Raman spectrum obtained from the surface of the liquid exposed to the atmosphere, the shoulder at 1010 cm^{-1} is missing on the low-frequency side of the intense band at 1023 cm^{-1}. The Raman spectrum obtained from the sample at the bottom of the tube is identical to the spectrum shown in Figure 3 because the bottom part of the sample was still relatively dry. It is also evident from Figure 11 that the ν(S−OH) mode at 850 cm^{-1} experiences blue shift of ~20 cm^{-1} in the sample exposed to moisture. The relative intensity of the ν_s(S═O) mode seen as a shoulder at 1046 cm^{-1} increases in the Raman spectrum obtained from the

dx.doi.org/10.1021/jp302091d | J. Phys. Chem. B 2012, 116, 7281−7290

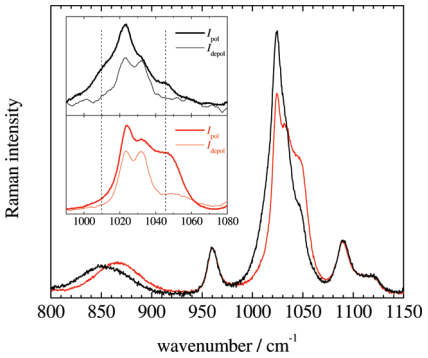

Figure 11. Raman spectra at room temperature and pressure of $[C_2C_1Im][HSO_4]$ in an open glass tube: the black line is the spectrum obtained by focusing the laser at the bottom of the tube, and the red line is the spectrum obtained by focusing the laser at the top of the sample near to the liquid surface exposed to moisture. The inset shows the 1000−1080 cm^{-1} range of polarized (bold lines) and depolarized (thin lines) Raman spectra corresponding to the black and red spectra of the main figure. Intensities of depolarized Raman spectra have been multiplied by 10. The vertical dashed lines at 1010 and 1046 cm^{-1} indicate the position of ν_s(S═O) modes in hydrogen-bonded anions forming chains and dimers, respectively.

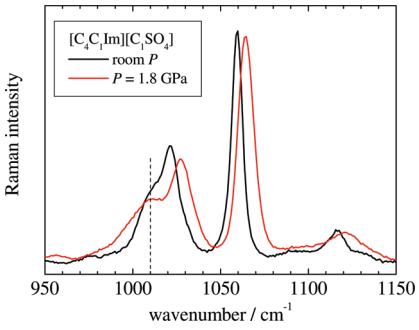

Figure 12. Raman spectra at room pressure (black) and 1.8 GPa (red) at room temperature in the range of the ν_s(S═O) mode of $[C_4C_1Im][C_1SO_4]$. The vertical dashed line indicates the position of the 1010 cm^{-1} band that is not shifted at high pressure.

surface of the liquid because this component is related to local structures of anions interacting with cations, water, or other anion in small structures like $(HSO_4^-)_2$ dimers.

The inset of Figure 11 highlights the 1000−1080 cm^{-1} range of the Raman spectra of $[C_2C_1Im][HSO_4]$ recorded with polarization selection for both the black and red curves of the main figure. This spectral range is strongly polarized, so that intensities of depolarized Raman spectra in Figure 11 have been multiplied by 10 for comparison purposes. The normal modes of the imidazolium ring at 1023 and 1034 cm^{-1} dominate the depolarized spectra. The Raman spectra of the wet part of the sample (red curves in the inset) show that the ν_s(S═O) mode in the polarized and depolarized spectrum is observed at 1046 and 1050 cm^{-1}, respectively. This is the so-called noncoincidence effect mentioned in section IIIA[43,36] that has been found in Raman spectra of concentrated aqueous solution of NH_4HSO_4.[22] The noncoincidence effect for the ν_s(S═O) mode at 1046 cm^{-1} provides further support for the proposition of short-range orientated structures of hydrogen-bonded HSO_4^- anions in the ionic liquid. In summary, Figure 11 is a nice illustration of absorption of water from the atmosphere by the surface of the ionic liquid $[C_2C_1Im][HSO_4]$. Proper to the small diameter of the glass tube and the high viscosity of the ionic liquid, it was possible to follow in a time interval of days the modification of Raman band shape of the ν_s(S═O) modes along the liquid column in the tube as water slowly went into the bulk of the liquid.

Handling the diamond anvil cell unfortunately does not prevent the sample from exposure to moisture, so that Raman spectra of the hygroscopic ionic liquids $[C_2C_1Im][HSO_4]$ or $[C_4C_1Im][HSO_4]$ obtained in the high-pressure cell indicated wet samples (like the spectrum of $[C_2C_1Im][HSO_4]$ shown by red line in Figure 11). On the other hand, the Raman spectrum of $[C_4C_1Im][C_1SO_4]$ in the diamond anvil cell with no applied pressure was essentially the same of Figure 3, so that we attempted an investigation of the pressure effect on $[C_4C_1Im][C_1SO_4]$. Figure 12 compares the ν_s(S═O) frequency range of Raman spectra of $[C_4C_1Im][C_1SO_4]$ at room pressure and 1.8 GPa. The ν_s(S═O) mode at 1010 cm^{-1} is clearly seen as a shoulder on the low-frequency side of the imidazolium ring band at 1023 cm^{-1}. Interestingly, whereas all bands experience blue shift of ∼5.0 cm^{-1} in this pressure range, the ν_s(S═O) mode at 1010 cm^{-1} becomes broader, but remains at the same wavenumber. We suggested that this unique behavior of the ν_s(S═O) mode at 1010 cm^{-1} is due to the relatively stable arrangement of hydrogen-bonded anions that makes the oscillator less prone to experience the effect of increasing density for the liquid under high pressure.

In summary, the ν_s(S═O) mode is a good vibrational probe of the environment experienced by HSO_4^- anions in ionic liquids. As previously found in crystalline phases of alkali HSO_4^- salts,[25−28] the ν_s(S═O) stretching mode gives two bands in Raman spectra of ionic liquids as the consequence of long and short structures of hydrogen-bonded anions. A first intuitive attempt to explain the origin of ionic liquids viscosity is the strength of anion−cation interactions. For instance, changing the anion from Cl^- to bis(trifluoromethylsulfonyl)-imide, $[(CF_3SO_2)_2N]^-$, while keeping the same $[C_4C_1Im]^+$ cation, the viscosity decreases by 3 orders of magnitude. The low viscosity of $[C_4C_1Im][(CF_3SO_2)_2N]$ arises from weak cation−anion interactions and conformational variety allowed by the complex anion.[55] An interesting finding is that methylation of the carbon atom $C_{(2)}$ of the imidazolium ring, resulting in the 1-butyl-2,3-dimethylimidazolium cation, while keeping the same anion, increases the viscosity in spite of blocking the main site of anion−cation hydrogen bond. The apparent counterintuitive result of a higher viscous liquid with the reduction of hydrogen bonding has been explained by a loss of configurational variation,[56] a more ordered Coulomb network,[57,58] or higher barrier of potential energy that restricts ionic mobility.[59] In contrast, the high viscosity of imidazolium ionic liquids with the HSO_4^- anion should not be assigned to a particularly strong imidazolium−HSO_4^- interaction in comparison with alkyl sulfate counterparts. It is worth noting that it is not only the strong interaction of the cation−anion pair that is playing a role on the high viscosity of, e.g., $[C_4C_1Im]Cl$ but also the cross-linking ability to develop a network of cation−anion−cation contacts.[55] In the case of HSO_4^- ionic liquids, extended structures of hydrogen-bonded anions result in a network of anions in the bulk, as previously suggested in simple high-temperature HSO_4^- molten salts based on alkali metal cations,[36] and consequently a very viscous melt.

dx.doi.org/10.1021/jp302091d | J. Phys. Chem. B 2012, 116, 7281−7290

IV. CONCLUSIONS

Raman spectra of $[C_2C_1Im][HSO_4]$ and $[C_4C_1Im][HSO_4]$ obtained in this work do not have bands of sulfuric acid as previously found in the Raman spectrum of $[C_6C_1Im][HSO_4]$.[18] Raman spectra of the alkyl sulfates counterparts $[C_2C_1Im][C_2SO_4]$ and $[C_4C_1Im][C_1SO_4]$ obtained in this work agree with previous works.[41,42] Vibrational frequencies of C−H stretching modes shift to higher wavenumber with increasing pressure with no indication of the red shift that has been interpreted as stabilization of cation−anion C—H···O hydrogen bonds in $[C_1C_1Im][C_1SO_4]$.[17] The doublet of bands above 3100 cm^{-1} is observed at the same position for ionic liquids with HSO_4^- or alkyl sulfate anions. The alternative interpretation of this spectral range as mixed states in Fermi resonance[14−16] is consistent with the pressure dependence of the Raman spectra. Nevertheless, the finding of essentially same vibrational frequencies of the imidazolium normal modes in ionic liquids with HSO_4^- or alkyl sulfates anions suggests there are no significant differences in anion−cation interactions that could be on the origin of the high viscosity of HSO_4^- ionic liquids.

Vibrational frequencies of the ν(S−OH) and ν_s(S═O) stretching modes of HSO_4^- in the ionic liquids are observed in the same wavenumbers as in the (high temperature) molten salt $KHSO_4$.[29,30] Two Raman bands at 1046 and 1010 cm^{-1} were assigned to ν_s(S═O) stretching modes of the HSO_4^- anion in ionic liquids. The lower frequency component corresponds to hydrogen-bonded anions forming structures like chains, $(HSO_4^-)_n$.[25−28] The component at 1046 cm^{-1} corresponds to HSO_4^- interacting with neighboring species, which can be imidazolium cations and also another HSO_4^- in structures like dimers, $(HSO_4^-)_2$. If the ionic liquid contained in an open glass tube is left exposed to water from atmosphere, the spectral signature of $(HSO_4^-)_n$ chains at 1010 cm^{-1} disappears, while the intensity of the ν_s(S═O) mode at 1046 cm^{-1} increases. Evidence of hydrogen-bonded anions has been also found for the ionic liquid containing the methyl sulfate anion, but not in the ethyl sulfate derivative. The ν_s(S═O) mode at 1010 cm^{-1} in the Raman spectrum of $[C_4C_1Im][C_1SO_4]$ does not shift as pressure increases, suggesting that hydrogen-bonded anions are forming relatively well optimized structures. In summary, a network of hydrogen-bonded anions is the origin of the high viscosity of HSO_4^- ionic liquids.

AUTHOR INFORMATION

Corresponding Author

*E-mail: mccribei@iq.usp.br.

Notes

The authors declare no competing financial interest.

ACKNOWLEDGMENTS

The author is indebted to FAPESP and CNPq for financial support.

REFERENCES

(1) Lewandowski, A.; Swiderska-Mocek, A. *J. Power Sources* **2009**, *194*, 601−609.
(2) Chen, R. J.; Zhang, H. Q.; Wu, F. *Prog. Chem.* **2011**, *23*, 366−373.
(3) Marciniak, A. *Fluid Phase Equilib.* **2010**, *294*, 213−233.
(4) Hubbard, C. D.; Illner, P.; van Eldik, R. *Chem. Soc. Rev.* **2011**, *40*, 272−290.
(5) Reichardt, C. *Green Chem.* **2005**, *7*, 339−351.
(6) Weingärtner, H. *Angew. Chem., Int. Ed.* **2008**, *47*, 654−670.
(7) Tokuda, H.; Hayamizu, K.; Ishii, K.; Susan, Md. A. B. H.; Watanabe, M. *J. Phys. Chem. B* **2005**, *109*, 6103−6110.
(8) Costa, A. J. L.; Esperança, J. M. S. S.; Marrucho, I. M.; Rebelo, L. P. N. *J. Chem. Eng. Data* **2011**, *56*, 3433−3441.
(9) Fernández, A.; García, J.; Torrecilla, J. S.; Oliet, M.; Rodriguéz, F. *J. Chem. Eng. Data* **2008**, *53*, 1518−1522.
(10) Kölle, P.; Dronskowski, R. *Inorg. Chem.* **2004**, *43*, 2803−2809.
(11) Holbrey, J. D.; Reichert, W. M.; Swatloski, R. P.; Broker, G. A.; Pitner, W. R.; Seddon, K. R.; Rogers, R. D. *Green Chem.* **2002**, *4*, 407−413.
(12) Berg, R. W. *Monat. Chem.* **2007**, *138*, 1045−1075.
(13) Monteiro, M. J.; Bazito, F. F. C.; Siqueira, L. J. A.; Ribeiro, M. C. C.; Torresi, R. M. *J. Phys. Chem. B* **2008**, *112*, 2102−2109.
(14) Lassègues, J.-C.; Grondin, J.; Cavagnat, D.; Johansson, P. *J. Phys. Chem. A* **2009**, *113*, 6419−6421.
(15) Wulf, A.; Fumino, K.; Ludwig, R. *J. Phys. Chem. A* **2010**, *114*, 685−686.
(16) Grondin, J.; Lassègues, J.-C.; Cavagnat, D.; Buffeteau, T.; Johansson, P.; Holomb, R. *J. Raman Spectrosc.* **2011**, *42*, 733−743.
(17) Chang, H.-C.; Jiang, J.-C.; Tsai, W.-C.; Chen, G.-C.; Lin, S. H. *J. Phys. Chem. B* **2006**, *110*, 3302−3307.
(18) Kiefer, J.; Pye, C. C. *J. Phys. Chem. A* **2010**, *114*, 6713−6720.
(19) Irish, D. E.; Chen, H. *J. Phys. Chem.* **1970**, *74*, 3796−3801.
(20) Turner, D. J. *J. Chem. Soc., Faraday Trans. 2* **1972**, *68*, 643−648.
(21) Dawson, B. S. W.; Irish, D. E.; Toogood, G. E. *J. Phys. Chem.* **1986**, *90*, 334−341.
(22) Rudolph, W. *Z. Phys. Chem.* **1996**, *194*, 73−95.
(23) Walrafen, G. E.; Yang, W.-H.; Chu, Y. C.; Hokmabadi, M. S. *J. Solution Chem.* **2000**, *29*, 905−936.
(24) Walrafen, G. E.; Yang, W.-H.; Chu, Y. C. *J. Phys. Chem. A* **2002**, *106*, 10162−10173.
(25) Goypiron, A.; Villepin, J.; Novak, A. *J. Raman Spectrosc.* **1980**, *9*, 297−303.
(26) Pham-Thi, M.; Colomban, Ph.; Novak, A.; Blinc, R. *J. Raman Spectrosc.* **1987**, *18*, 185−194.
(27) Colomban, Ph.; Pham-Thi, M.; Novak, A. *Solid State Ionics* **1987**, *24*, 193−203.
(28) Varma, V.; Rangavittal, N.; Rao, C. N. R. *J. Solid State Chem.* **1993**, *106*, 164−173.
(29) Walrafen, G. E.; Irish, D. E.; Young, T. F. *J. Chem. Phys.* **1962**, *37*, 662−670.
(30) Fehrmann, R.; Hansen, N. H.; Bjerrum, N. J. *Inorg. Chem.* **1983**, *22*, 4009−4014.
(31) Cotton, F. A.; Frenz, B. A.; Hunter, D. L. *Acta Crystallogr. B* **1975**, *31*, 302−304.
(32) Payan, F.; Haser, R. *Acta Crystallogr. B* **1976**, *32*, 1875−1879.
(33) Sonneveld, E. J.; Visser, J. W. *Acta Crystallogr. B* **1979**, *35*, 1975−1977.
(34) Itoh, K.; Ozaki, T.; Nakamura, E. *Acta Crystallogr. B* **1981**, *37*, 1908−1909.
(35) Jirák, Z.; Dlouhá, M.; Vratislav, S.; Balagurov, A. M.; Beskrovnyi, A. I.; Gordelii, V. I.; Datt, I. D.; Shuvalov, L. A. *Phys. Status Solidi* **1987**, *100*, 117−122.
(36) Rogers, S. E.; Ubbelohde, A. R. *Trans. Faraday Soc.* **1950**, *46*, 1051−1061.
(37) Fredlake, C. P.; Crosthwaite, J. M.; Hert, D. G.; Aki, S. N. V. K.; Brennecke, J. F. *J. Chem. Eng. Data* **2004**, *49*, 954−964.
(38) Mudring, A.-V. *Aust. J. Chem.* **2010**, *63*, 544−564.
(39) Aparicio, S.; Atilhan, M.; Karadas, F. *Ind. Eng. Chem. Res.* **2010**, *49*, 9580−9595.
(40) (a) Ribeiro, M. C. C. *J. Chem. Phys.* **2010**, *132*, 024503;(b) **2011**, *134*, 244507.
(41) Kiefer, J.; Fries, J.; Leipertz, A. *Appl. Spectrosc.* **2007**, *61*, 1306−1311.
(42) Dhumal, N. R.; Kim, H. J.; Kiefer, J. *J. Phys. Chem. A* **2011**, *115*, 3551−3558.
(43) Logan, D. E. *Chem. Phys.* **1986**, *103*, 215−225.
(44) Torii, H.; Tasumi, M. *J. Chem. Phys.* **1993**, *99*, 8459−8465.

(45) Wallen, S. L.; Nikiel, L.; Yi, J.; Jonas, J. *Chem. Phys. Lett.* **1994**, *229*, 82−86.
(46) Brodin, A.; Jacobsson, P. *J. Mol. Liq.* **2011**, *164*, 17−21.
(47) Aoki, K.; Yamawaki, H.; Sakashita, M. *Science* **1995**, *268*, 1322−1324.
(48) Devendorf, G. S.; Hu, M.-H. A.; Ben-Amotz, D. *J. Phys. Chem. A* **1998**, *102*, 10614−10619.
(49) Arencibia, A.; Taravillo, M.; Caceres, M.; Nunez, J.; Baonza, V. G. *J. Chem. Phys.* **2005**, *123*, 214502.
(50) Jiang, X. L.; Zhou, M.; Li, Z. W.; Sun, C. L.; Gao, S. Q. *J. Appl. Phys.* **2011**, *110*, 113101.
(51) Takekiyo, T.; Imai, Y.; Hatano, N.; Abe, H.; Yoshimura, Y. *Chem. Phys. Lett.* **2011**, *511*, 241−246.
(52) Okajima, H.; Hamaguchi, H. *Chem. Lett.* **2011**, *40*, 1308−1309.
(53) Holom, R; Martinelli, A.; Albinsson, I.; Lassegues, J. C.; Johansson, P.; Jacobsson, P. *J. Raman Spectrosc.* **2008**, *39*, 793−805.
(54) Lassegues, J. C.; Grondin, J.; Holomb, R.; Johansson, P. *J. Raman Spectrosc.* **2007**, *38*, 551−558.
(55) Hunt, P. A.; Gould, I. R.; Kirchner, B. *Aust. J. Chem.* **2007**, *60*, 9−14.
(56) Hunt, P. A. *J. Phys. Chem. B* **2007**, *111*, 4844−4853.
(57) Fumino, K.; Wulf, A.; Ludwig, R. *Angew. Chem., Int. Ed.* **2008**, *47*, 8731−8734.
(58) Noack, K.; Schulz, P. S.; Paape, N.; Kiefer, J.; Wasserscheid, P.; Leipertz, A. *Phys. Chem. Chem. Phys.* **2010**, *12*, 14153−14161.
(59) Izgorodina, I. E.; Maganti, R.; Armel, V.; Dean, P. M.; Pringle, J. M.; Seddon, K. R.; MacFarlane, D. R. *J. Phys. Chem. B* **2011**, *115*, 14688−14697.